

Photonic band gap effects on spontaneous emission lifetimes of an assembly of atoms in two-dimensional photonic crystals

Yun-Song Zhou,¹ Xue-Hua Wang,^{2,*} Ben-Yuan Gu,^{2,†} and Fu-He Wang¹

¹*Department of Physics, Capital Normal University, Beijing 100037, China and*

²*Institute of Physics, Chinese Academy of Sciences, P.O.Box 603, Beijing 100080, China*

(Received 7 December 2004; revised manuscript received 9 May 2005; published 15 July 2005)

The lifetime distribution functions of the spontaneous emission (SE) of the excited atoms embedded in two-dimensional (2D) photonic crystals (PCs) with square lattice, consisting of square air rods in dielectric medium with different filling factors, are calculated by using the plane wave expansion method. The numerical results show that the SE in the 2D PCs cannot be prohibited completely but it can be inhibited intensively by the pseudo-PBG of the PCs. In the pseudoband edges, the SE is accelerated obviously. The reduced average lifetime of the excited atoms and the extension of the reduced lifetime distribution in the 2D PCs both are the same as those in the 3D PCs in the order of magnitude. Our results provide an available way to control the behavior of the SE by changing the structures of the 2D PCs.

DOI: [10.1103/PhysRevE.72.017601](https://doi.org/10.1103/PhysRevE.72.017601)

PACS number(s): 42.70.Qs, 32.80.-t, 42.50.-p

The spontaneous emission (SE) lifetime of an excited atom located in structural material environment is quite different from that in free space because of different zero-point fluctuations of the electromagnetic fields at different positions of the atom [1]. The photonic crystals (PCs), proposed first by Yablonovitch [2] and John [3], have offered a unique way to investigate the SE in structural materials. One of the most important features of PCs is photonic band gap (PBG) structure. The SE in three-dimensional (3D) PCs can be suppressed when atomic transition frequency just falls inside a PBG. On the other hand, if the atomic transition frequency takes an appropriate value, for instance, near the band edge which corresponds to large local density of states (LDOS), thus the SE rate is significantly enhanced. It implies that the SE rate can be modified by changing the PC structures. Therefore, the investigations of the behavior of the SE in the PCs become an interesting issue [4–18]. The experimental studies on the SE in the 3D PCs have been achieved [4,5]. In these experiments the wide lifetime distributions were observed. There exhibits the coexistence of both the accelerated and the inhibited decay processes in the PCs. As a result, the conventional concept of a single-averaged lifetime of the SE is invalid in the PCs [16].

For describing the lifetime distribution of the SE caused by the effect of PC and investigating the dynamic decay processes of the SE, Wang *et al.* defined the lifetime distribution function (LDF) theoretically [16]. The numerical result shows a spread of LDFs over a wide range, including both the inhibited and the accelerated decay processes of atoms in the 3D PC. After that, as an available concept, the LDF has been used to study the SE behavior of atoms in the dielectric sandwich structures successfully [19,20].

Two-dimensional (2D) PCs have also been received much attention because of their easy fabrication and having the light-guiding ability [21]. Recently, the properties of the SE

and lifetime distribution in the 2D PCs have been examined by calculating the 2D LDOS in the PCs that possess absolute PBG [22]. However, as 2D PCs have translation invariance along the height direction of the scattering rods, thus, the SE in the 2D PCs may not be forbidden completely because the SE light may travel along the height direction of the rods and escape out of the 2D plane. Therefore, the properties of SE in the 2D PCs are governed by the actual 3D LDOS of the 2D PCs, rather than the 2D LDOS. Only pseudo-PBGs exist in the 2D PCs. It is worth pointing out that the absolute or complete PBGs exist only when the propagation of light waves is fully restricted to the periodical structural plane of the 2D PCs. But this is impossible for the SE light in the 2D PCs. Consequently, it is expected that the SE should be partially suppressed or enhanced in this system. In the present paper, we explore the SE properties of an assembly of atoms embedded in the 2D PCs by calculating the actual 3D LDOS and investigate the effects of the pseudo-PBGs in the 2D PCs on the LDFs. Our attention focuses on two special frequencies: one is inside the pseudo-PBG and the other is at the pseudo-band edge.

The LDF is defined as [16,19]

$$\rho(\tilde{\tau}, \omega) = \sum_i W_i \frac{1}{\sqrt{\pi}\sigma} \exp\left[-\frac{[\tilde{\tau} - \tilde{\tau}(\mathbf{r}_i, \omega)]^2}{\sigma^2}\right], \quad (1)$$

where $\tilde{\tau}(\mathbf{r}_i, \omega) = \tau(\mathbf{r}_i, \omega) / \tau_f(\omega)$, $\tau(\mathbf{r}_i, \omega)$ and $\tau_f(\omega)$ are the SE lifetimes at a given position \mathbf{r}_i in the PC and in homogeneous medium, respectively. W_i denotes the weight factor. In the cases of homogeneous distribution of atoms in space and the random orientation of the dipole moment $W_i = 1$. The summation runs over all the considered excited atoms, where we choose $\sigma = 0.05$ that is enough to guarantee the smoothness of the LDF curves. $\tau(\mathbf{r}_i, \omega)$ is given by the following equation [23]:

*Email address: wangxh@aphy.iphy.ac.cn

†Email address: guby@aphy.iphy.ac.cn

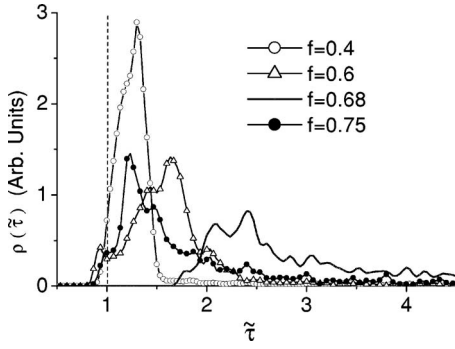


FIG. 1. LDFs in dielectric background medium of the PCs in 2D square lattice, consisting of air square rods in the background medium of $\epsilon=12.96$ with different filling factors $f=0.4, 0.6, 0.68,$ and 0.75 . The transition frequency of atoms sets as $\omega_g=0.425(2\pi c/a)$.

$$\tau(\mathbf{r}, \omega) = \left[\frac{\pi \omega_0^2 u_d^2}{3 \epsilon_0 \hbar \omega} \mathcal{D}_{\text{LDOS}}(\mathbf{r}, \omega) \right]^{-1}, \quad (2)$$

where ω_0 denotes the atomic transition frequency and u_d is the dipole moment of atom. The local density of photonic states is defined as

$$\mathcal{D}_{\text{LDOS}}(\omega, \mathbf{r}) = \frac{1}{(2\pi)^3} \sum_n \int_{\text{FBZ}} d\mathbf{k} |\mathbf{E}_{n\mathbf{k}}(\mathbf{r})|^2 \delta(\omega - \omega_{n\mathbf{k}}), \quad (3)$$

where $\omega_{n\mathbf{k}}$ and $\mathbf{E}_{n\mathbf{k}}(\mathbf{r})$ are the eigenfrequency and eigenmode of the electric fields in the PC, respectively. They are calculated by using the plane wave expansion method and automatically satisfy the orthonormal conditions (see Appendix)

By inserting Eqs. (2) and (3) into Eq. (1), the LDF can be evaluated numerically. First, we consider a 2D square lattice PC composed of square air rods in the dielectric medium of the dielectric constant $\epsilon=12.96$. Each square rod is rotated an angle of $\theta=30^\circ$ around its symmetric axis in the height direction. In the following calculations, all the above structural parameters are fixed except for different filling factors of $f=0.4, 0.6, 0.68,$ and 0.75 . It should be pointed out that in the case of $f=0.68$, this PC belongs to an optimal structure because it possesses a largest pseudo-PBG of $\Delta\omega=0.063(2\pi c/a)$ (here a denotes the lattice constant and c the light speed in vacuum) with a midgap frequency of $\omega_g=0.425(2\pi c/a)$ [24–26]. So, we pay attention to two spacial frequencies: the midgap of $\omega_g=0.425(2\pi c/a)$ and the pseudoband edge of $\omega_e=0.385(2\pi c/a)$.

The LDFs of the excited atoms located in the background medium are displayed in Fig. 1 when the atomic transition frequency is $\omega=\omega_g=0.425(2\pi c/a)$ for $f=0.4, 0.6, 0.68$ and 0.75 . In order to reveal the pure photonic crystal effect, the reference lifetime τ_f chooses that when atoms are embedded in homogeneous background medium of $\epsilon=12.96$, which is shown by the vertical dashed-line located at $\tilde{\tau}=1$. The curve of $f=0.68$ corresponds to the LDF of the optimal structural sample. The largest filling factor $f=0.75$ in the structure just corresponds to the overlap of the nearest air rods. Two notable results can be observed from Fig. 1: (i) the LDF in each case has quite wide distribution. It implies that the SE behavior in the 2D PCs is no longer described by a single

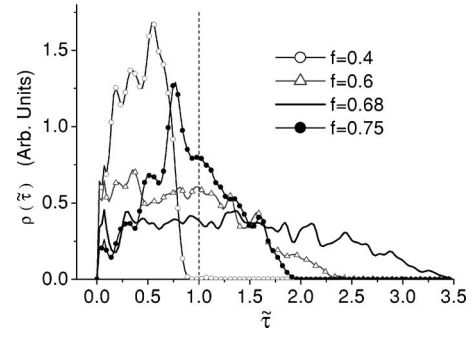


FIG. 2. LDFs in the air square rods for the atomic transition frequency of $\omega_g=0.425(2\pi c/a)$. All other parameters are chosen the same as those in Fig. 1.

lifetime, similar to the result in the 3D PCs, as reported in Ref. [16]. (ii) Compared with the case of the atoms in the homogeneous medium of $\epsilon=12.96$, all the SEs almost are inhibited. The SE lifetimes gradually become long as f increases from 0.4 to 0.68 . But when $f=0.75$, the inhibition effect of the SE in the PC is weakened. These results can be well understood when we note that the structure of $f=0.68$ possesses the largest pseudo-PBG and the atomic transition frequency is just located at the center of the largest pseudo-PBG. When the filling factor goes away from $f=0.68$, the width of the pseudo-PBG of the corresponding PC is narrowed down and the atomic transition frequency deviates from the center of the pseudo-PBG. Therefore, the inhibition effect of the SE in the non-optimal structures is significantly weakened.

We also calculate the LDFs of the atoms which are placed within the air rods for different filling factors as shown in Fig. 2. The parameters remain unchanged. The reference lifetime chooses that of atoms in vacuum in order to reveal the PC effect. All the curves show quite wide lifetime distribution, as illustrated in Fig. 1. Two differences from Fig. 1 should be addressed: One is that for the structure of $f=0.4$, the reduced lifetimes almost distribute in the range of $\tilde{\tau}<1$, which manifests that the most SEs now are accelerated. The other is that for the structures of $f=0.6, 0.68$ and 0.75 , the lifetimes of some atoms are decreased and the others are increased, which reveals that both the acceleration and the inhibition processes coexist in these PC samples. It is no surprising that the considerable difference occurs in Figs. 1 and 2. The electric fields of the eigen modes are discontinuous at interfaces, for instance, the electric fields in the air rods are larger than that in the dielectric medium. This leads to sudden enhancement of the LDOS near interfaces in the air rods, which gives rise to the inhibition or acceleration process of the SE in the high or low refractive index medium. Combining with the position-dependent fluctuations of the LDOS, these results in Fig. 2 can be well understood.

We now turn to examine the case of $\omega=\omega_e=0.385(2\pi c/a)$, i.e. the atomic transition frequency is located at the pseudoband edge of the optimal structural sample of $f=0.68$. The numerical results of the LDFs are displayed in Fig. 3 when the atoms are randomly spread in the dielectric background medium, where the reference lifetime is the same as that in Fig. 1. The curve of $f=0.68$ shows

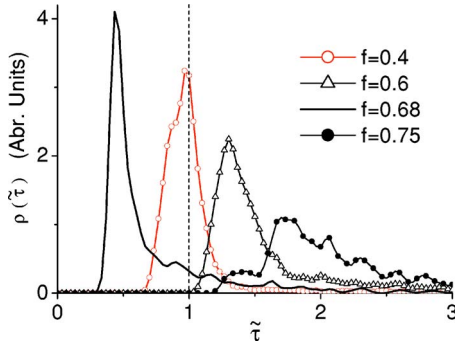


FIG. 3. (Color online) Same as Fig. 1 except for the atomic transition frequency of $\omega_e = 0.385(2\pi c/a)$.

that the lifetime distribution becomes narrow and the SEs almost are accelerated. As it is well-known that in the 3D PCs the band edges enhance the SE because the LDOS reach its maximum near the band edges. It is reasonable to expect that the pseudoband edges of 2D PCs have similar effect. On the other hand, for other three structures, the atomic transition frequency goes away from the pseudoband edges of these structures, thus, the LDOS is reduced and the pseudoband edge effect is substantially weakened. In addition, high refractive index of the dielectric medium also leads to the reduction of the LDOS, which results in the suppression of the SE process. Consequently, for the other three structures, the SE enhanced effect should be gradually weakened, i.e., the SE suppression effect becomes dominant. These arguments are just confirmed by the results displayed in Fig. 3. The LDFs of the atoms embedded in air rods for atomic transition frequency of $\omega = 0.385(2\pi c/a)$ are shown in Fig. 4. The reference lifetime is the same as that in Fig. 2. Except for the sample of $f=0.6$, the SEs of atoms in the other samples are accelerated. Among them, the SE enhanced effect in the optimal structure of $f=0.68$ is most remarkable due to the presence of a large LDOS in the air rods caused by the pseudoband edge and the dielectric discontinuity. The curve of 0.75 in Fig. 4 is different from the corresponding curves in Fig. 2. It does not contain any inhibition component of the SE because the transition frequency of $\omega = 0.385(2\pi c/a)$ is located outside pseudo-PBGs, thus, the inhibition process can not occur. Why does the curve of $f=0.6$ lie across the dashed line with a wide profile? We cal-

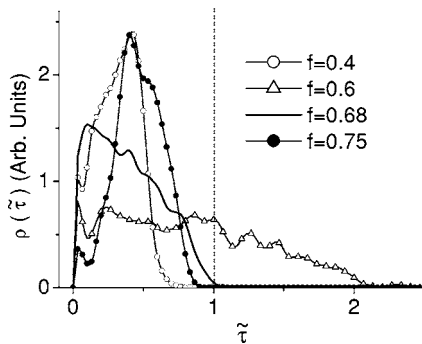


FIG. 4. Same as Fig. 2 except for the atomic transition frequency of $\omega_e = 0.385(2\pi c/a)$.

culate the pseudo-PBG for this PC sample and find that its pseudo-PBG spreads over the frequency range of $[0.375, 0.395](2\pi c/a)$. The atomic transition frequency $\omega = 0.385(2\pi c/a)$ falls within the pseudo-PBG. So both the enhanced effect caused by the dielectric discontinuity and the inhibition effect generated from the pseudo-PBG coexist, similar to the case appearing in Fig. 2.

Here we prefer to compare our results with that of 3D PCs, as reported in Ref. [16], we find the lifetime distribution widths in the 2D PCs have the same order of magnitude as that in the 3D PCs. As the fabrication of the 2D PCs with high index contrast is easier than that of the 3D PCs, our results may provide a useful way to observe the SE inhibition and enhancement effects in the PCs, experimentally.

In summary, we have calculated the LDFs in the 2D PCs by considering the actual 3D LDOS. The numerical results show that the SE cannot be prohibited completely but it can be inhibited intensively by pseudo-PBGs in the 2D PCs. In the pseudoband edges, the SE can be accelerated apparently. Our results may offer an available way to control the behavior of the SE by modifying the structures of the 2D PCs.

This work was supported by Chinese National Key Basic Research Special Fund and by Natural Science Foundation of Beijing, China.

APPENDIX

For 2D PC, the following orthonormal conditions are applied:

$$\begin{aligned} \frac{1}{(2\pi)^3} \int_{-\infty}^{\infty} dz \int_{R^2} d\mathbf{r}_{xy} \mathbf{H}_{n\mathbf{k}}(\mathbf{r}) \cdot \mathbf{H}_{n'\mathbf{k}'}^*(\mathbf{r}) \\ = \delta(k_z - k'_z) \delta(\mathbf{k}_{xy} - \mathbf{k}'_{xy}) \delta_{nn'}, \end{aligned} \quad (\text{A1})$$

$$\begin{aligned} \frac{1}{(2\pi)^3} \int_{-\infty}^{\infty} dz \int_{R^2} d\mathbf{r}_{xy} \epsilon(\mathbf{r}) \mathbf{E}_{n\mathbf{k}}(\mathbf{r}) \cdot \mathbf{E}_{n'\mathbf{k}'}^*(\mathbf{r}) \\ = \delta(k_z - k'_z) \delta(\mathbf{k}_{xy} - \mathbf{k}'_{xy}) \delta_{nn'}, \end{aligned} \quad (\text{A2})$$

where S_u is the area of a 2D primitive cell. In our calculations, Eqs. (A1) and (A2) are automatically satisfied. Here, we give a derivation for them. First, we numerically solve the Hermite eigen equation of magnetic field $H_{n\mathbf{k}}(\mathbf{r})$

$$\nabla \times [\epsilon^{-1}(\mathbf{r}) \nabla \times \mathbf{H}_{n\mathbf{k}}(\mathbf{r})] = \left(\frac{\omega_{n\mathbf{k}}}{c} \right)^2 \mathbf{H}_{n\mathbf{k}}(\mathbf{r}) \quad (\text{A3})$$

and then the electric field modes are obtained by

$$\mathbf{E}_{n\mathbf{k}}(\mathbf{r}) = \frac{ic}{\omega_{n\mathbf{k}} \epsilon(\mathbf{r})} \nabla \times \mathbf{H}_{n\mathbf{k}}(\mathbf{r}). \quad (\text{A4})$$

We expand the magnetic field and the dielectric constant by the plane waves

$$\mathbf{H}_{n\mathbf{k}}(\mathbf{r}) = \sum_{\mathbf{G}} \mathbf{H}_{n\mathbf{k}}(\mathbf{G}) e^{i(\mathbf{G} + \mathbf{k}_{xy}) \cdot \mathbf{r}_{xy}} e^{ik_z z}, \quad (\text{A5})$$

$$\epsilon^{-1}(\mathbf{r}_{xy}) = \sum_{\mathbf{G}} \epsilon^{-1}(\mathbf{G}) e^{(\mathbf{G}) \cdot \mathbf{r}_{xy}}, \quad (\text{A6})$$

where \mathbf{G} is a 2D reciprocal lattice vector, $\mathbf{k} = \mathbf{k}_{xy} + k_z \hat{z}$ and \mathbf{k}_{xy} is a wave vector in 2D Brillouin zone. Inserting Eqs. (A5) and (A6) into Eq. (A3):

$$\begin{aligned} & \sum_{\mathbf{G}'} \epsilon^{-1}(\mathbf{G} - \mathbf{G}') (\mathbf{k} + \mathbf{G}) \times [\mathbf{H}_{n\mathbf{k}}(\mathbf{G}') \times (\mathbf{k} + \mathbf{G}')] \\ &= \left(\frac{\omega_{n\mathbf{k}}}{c} \right)^2 \mathbf{H}_{n\mathbf{k}}(\mathbf{G}). \end{aligned} \quad (\text{A7})$$

This is a typical eigenvalue problem of a Hermite matrix. The standard codes automatically give orthonormal eigen vectors, i.e.,

$$\sum_{\mathbf{G}} \mathbf{H}_{n\mathbf{k}}(\mathbf{G}) \cdot \mathbf{H}_{n'\mathbf{k}}^*(\mathbf{G}) = \delta_{nn'}. \quad (\text{A8})$$

Let the PC be periodic with respect to x and y with periods p_x and p_y ($p_x p_y = S_u$), respectively. According to the Bloch theorem, when $\mathbf{r} = \mathbf{r}_{xy}$, the $\mathbf{H}_{n\mathbf{k}}(\mathbf{r}_{xy})$ in Eq. (A3) is of the property

$$\mathbf{H}_{n\mathbf{k}}(\mathbf{r}_{xy} + m_x p_x + m_y p_y) = e^{i[k_x m_x p_x + k_y m_y p_y]} \mathbf{H}_{n\mathbf{k}}(\mathbf{r}_{xy}), \quad (\text{A9})$$

where m_x and m_y are integers. Then

$$\begin{aligned} & \int_{-\infty}^{\infty} dz \int_{R^2} d\mathbf{r}_{xy} \mathbf{H}_{n\mathbf{k}}(\mathbf{r}) \cdot \mathbf{H}_{n'\mathbf{k}'}^*(\mathbf{r}) \\ &= \int_{-\infty}^{\infty} e^{i(k_z - k'_z)z} dz \sum_{m_x, m_y} e^{i[(k_x - k'_x)m_x p_x + (k_y - k'_y)m_y p_y]} \\ & \quad \times \int_{S_u} d\mathbf{r}_{xy} \mathbf{H}_{n\mathbf{k}}(\mathbf{r}_{xy}) \cdot \mathbf{H}_{n'\mathbf{k}'}^*(\mathbf{r}_{xy}) \\ &= \frac{(2\pi)^3}{S_u} \delta(\mathbf{k} - \mathbf{k}') \int_{S_u} d\mathbf{r}_{xy} \mathbf{H}_{n\mathbf{k}}(\mathbf{r}_{xy}) \cdot \mathbf{H}_{n'\mathbf{k}'}^*(\mathbf{r}_{xy}). \end{aligned} \quad (\text{A10})$$

Inserting Eq. (A5) into Eq. (A10) and using Eq. (A8)

$$\frac{1}{(2\pi)^3} \int_{-\infty}^{\infty} dz \int_{R^2} d\mathbf{r}_{xy} \mathbf{H}_{n\mathbf{k}}(\mathbf{r}) \cdot \mathbf{H}_{n'\mathbf{k}'}^*(\mathbf{r}) = \delta(\mathbf{k} - \mathbf{k}') \delta_{nn'}. \quad (\text{A11})$$

Equation (A11) is Eq. (A1).

Using Eq. (A4) and noting that

$$\begin{aligned} & [\mathbf{H}_{n\mathbf{k}}(\mathbf{G}) \times (\mathbf{k} + \mathbf{G}) \cdot [\mathbf{H}_{n'\mathbf{k}'}(\mathbf{G}') \times (\mathbf{k} + \mathbf{G}')] \\ &= \mathbf{H}_{n\mathbf{k}}(\mathbf{G}) \cdot \{(\mathbf{k} + \mathbf{G}) \times [\mathbf{H}_{n'\mathbf{k}'}(\mathbf{G}') \times (\mathbf{k} + \mathbf{G}')]\}, \end{aligned} \quad (\text{A12})$$

Eq. (A2) may also be proved in a similar way.

-
- [1] E. M. Percell, Phys. Rev. **69**, 681 (1946).
 [2] E. Yablonovitch, Phys. Rev. Lett. **58**, 2059 (1987).
 [3] S. John, Phys. Rev. Lett. **58**, 2486 (1987).
 [4] J. Martorell and N. M. Lawandy, Phys. Rev. Lett. **65** 1877 (1990).
 [5] E. P. Petrov *et al.*, Phys. Rev. Lett. **81**, 77 (1998); M. Megens *et al.*, Phys. Rev. A **59**, 4727 (1999); M. Megens *et al.*, Phys. Rev. Lett. **83**, 5401 (1999); E. P. Petrov *et al.*, *ibid.* **83**, 5402 (1999).
 [6] S. John and J. Wang, Phys. Rev. Lett. **64**, 2418 (1990); Phys. Rev. B **43**, 12 772 (1991).
 [7] A. G. Kofman, G. Kurizki, and B. Sherman, J. Mod. Opt. **41**, 353 (1994).
 [8] S. Bay, P. Lambropoulos, and K. Molmer, Phys. Rev. Lett. **79**, 2654 (1997); Phys. Rev. A **55**, 1485 (1997).
 [9] S. John and T. Quang, Phys. Rev. A **50**, 1764 (1994); T. Quang and S. John, *ibid.* **56**, 4273 (1997).
 [10] S. Y. Zhu, H. Chen, and H. Huang, Phys. Rev. Lett. **79**, 205 (1997); **84**, 2136 (2000); Y. Yang, S. Y. Zhu, M. Zheng, and M. S. Zubairy, Phys. Rev. A **62**, 013805 (2000).
 [11] N. Vast, S. Jonh, and E. Busch Phys. Rev. A **65**, 043808 (2002).
 [12] I. Alvarado-Rodriguez, P. Halevi, and A. S. Sanchez, Phys. Rev. E **63**, 056613 (2001).
 [13] J. P. Dowling and C. M. Bowden, Phys. Rev. A **46**, 612 (1992).
 [14] H. P. Urbach and G. L. J. A. Rikken, Phys. Rev. A **57**, 3913 (1998).
 [15] R. Sprik, B. A. Van Tiggelen, and A. Lagendijk, Europhys. Lett. **35**, 265 (1996).
 [16] Xue-Hua Wang, Rong-Zhou Wang, Ben-Yuan Gu, and Guo-Zhen Yang, Phys. Rev. Lett. **88**, 093902 (2002).
 [17] Xue-Hua Wang, Ben-Yuan Gu, Rong-Zhou Wang, and Hong-Qi Xu, Phys. Rev. Lett. **91**, 113904 (2003).
 [18] R. C. McPhedran, L. C. Botten, J. McOrist, A. A. Asatryan, C. M. de Sterke, and N. A. Nicorovici, Phys. Rev. E **69**, 016609 (2004).
 [19] Fu-He Wang, Xue-Hua Wang, Ben-Yuan Gu, and Yun-Song Zhou, Phys. Rev. A **67**, 035802 (2003).
 [20] Lu Zhou and Gaoxiang Li, Opt. Commun. **230**, 347 (2004).
 [21] A. Mekis, J. C. Chen, I. Kurland, S. Fan, P. R. Villeneuve, and J. D. Joannopoulos, Phys. Rev. Lett. **77**, 3787 (1996).
 [22] Yong Zeng, Xiaoshuang Chen, and Wei Lu, Phys. Rev. E **70**, 047601 (2004).
 [23] Rong-Zhou Wang, Xue-Hua Wang, Ben-Yuan Gu, and Guo-Zhen Yang, Phys. Rev. B **67**, 155114 (2003).
 [24] Yun-Song Zhou, Ben-Yuan Gu, and Fu-He Wang, J. Phys.: Condens. Matter **15**, 4109 (2003).
 [25] Yun-Song Zhou, Ben-Yuan Gu, and Fu-He Wang, Eur. Phys. J. B **37**, 293 (2004).
 [26] Rong-Zhou Wang, Xue-Hua Wang, Ben-Yuan Gu, and Guo-Zhen Yang, J. Appl. Phys. **90**, 4307 (2001).